Continuous-Wave Mid-Infrared Gas Fiber Lasers

Mengrong Xu [iD], Fei Yu [iD], Muhammad Rosdi Abu Hassan [iD], and Jonathan C. Knight

Abstract—**Efficient continuous-wave laser emission of acetylene molecules at 3.1 μm wavelength has been demonstrated in low-loss hollow-core fiber by optically pumping using a fiber-amplified diode laser around 1.53 μm. In this paper, we report and compare the continuous-wave laser performance of acetylene molecules in the cavity and single-pass configurations. The use of low-loss antiresonant hollow-core fiber makes the single-pass configuration ideal for high-power laser generation and enables over 1.1 W continuous-wave mid-infrared laser output with over 33% slope efficiency relative to the absorbed pump power. The systematic characterization of power-scaling and pump power absorption properties demonstrates that the molecular kinetics inside hollow-core fiber determines the laser performance, and that low fiber attenuation is key to high-efficiency continuous-wave output.**

Index Terms—Optical fibers, optical fiber lasers, gas lasers .

I. INTRODUCTION

MID-INFRARED fiber lasers with high output powers have developed rapidly in recent years thanks to the maturing fabrication of soft glass and soft-glass fiber, as well as the advanced fiber laser technologies proven in the development of near-infrared fiber lasers [1]–[3]. At mid-infrared wavelengths above 3 μm, rare-earth-doped silica and silicate fibers fail to provide the efficient laser operation which they deliver at near-infrared wavelengths due to the high material loss as a result of strong phonon absorption at these longer wavelengths [4]. Although inferior to silica/silicate glasses as laser host glasses in terms of mechanical strength, chemical durability, thermal conductivity, and optical nonlinearity, the soft glasses, e.g., chalcogenide, telluride and fluoride glasses, offer advantages as host materials because of their lower phonon energies [2], [5].

Among many soft-glass fiber lasers, Erbium-doped fluoride fiber lasers have been demonstrated as the most successful candidate for high-power mid-infrared fiber lasers, being used to generate 30 Watt mid-infrared laser output at wavelengths near 3 μm [1]–[3], [6]–[9], with a predicted potential exceeding the 100 W power level [9]. By using a dual wavelength pumping scheme, watt-level fiber laser output can be achieved at longer

M. Xu, F. Yu, and J. C. Knight are with the Department of Physics, Centre for Photonics and Photonic Materials, University of Bath, Bath BA2 7AY, U.K. (e-mail: mx300@bath.ac.uk; fy230@bath.ac.uk; j.c.knight@bath.ac.uk).

M. R. A. Hassan was with the Department of Physics, University of Bath, Bath BA2 7AY, U.K. He is now with the Faculty of Engineering, Multimedia University, Cyberjaya 63100, Malaysia (e-mail: muhdrosdi22@gmail.com).

wavelengths up to 3.55 μm [10]. The outstanding performance of fluoride fiber lasers is attributed to the high achievable doping level up to 10 mol%, the relatively high mechanical strength, and low material loss (<0.05 dB/m) [1]. However, the overall progress of mid-infrared fiber lasers towards higher power output and longer wavelength extension is ultimately challenged in numerous ways, e.g., the typically high quantum defect, thermal management and fiber failure [2], some of which originate from the host materials. As an alternative technology, novel gas-filled hollow-core fiber lasers [11] based on the use of low-loss hollow-core fibers (HCFs) formed from silica and transmitting into the mid-infrared are free of those limitations and have demonstrated potential for high-power mid-infrared laser emission [12], [13]. They provide an alternative route to developing versatile high-power mid-infrared fiber lasers.

A. Low-Loss Hollow-Core Fibers

In 1999, the first hollow-core photonic bandgap fiber was demonstrated [14] and since then, the concept of hollow-core fibers (HCFs) [15] has been demonstrated to have the potential to greatly improve fiber performance, e.g., higher damage threshold, and reduced fiber nonlinearity and dispersion. The low-loss window of HCFs has been shown to extend from the mid-infrared spectral region to the near infrared and visible [16], [17]; meanwhile the attenuation record of HCFs is around 1 dB/km at 1.55 μm [16], approaching (although not yet quite competitive with) the best conventional silica fibers [18].

Recently, a modified design of low-loss HCF has emerged known as anti-resonant hollow-core fibers [19], characterized by an anti-resonant core wall with negative curvature. In contrast to the earlier photonic bandgap fibers this design offers several low-loss transmission windows and a larger core size. Because of the very low overlap of the light in the core with the material forming the cladding [20], [21], anti-resonant HCFs made from silica glass overcome the phonon barrier and exhibit excellent low-loss transmission at 3 μm wavelength [22], [23]. A minimum attenuation of 25 dB/km at 3 μm wavelength was reported [23]. The absorption of bulk silica is above 50 dB/m [4] at this wavelength, but the attenuation of the silica-based anti-resonant HCF is competitive with the best soft-glass fibers in this wavelength range [5], [24], [25]. In 2013, a low-loss anti-resonant HCF was successfully demonstrated in high energy (up to 195 mJ) pulsed laser delivery at 2.94 μm wavelength [26]. The large-core anti-resonant design makes the performance of anti-resonant HCFs far exceed its photonic bandgap counterpart in terms of damage threshold and fiber attenuation at long wavelengths [27]. More importantly, by proper design, single-mode performance can be obtained in anti-resonant HCF by using

phase matching [28]; higher-order modes are quickly dissipated in a short length by coupling to cladding modes with higher attenuation.

B. Traditional Optically-Pumped Gas Lasers

Optically-pumped molecular gas lasers are a convenient and versatile coherent source for the spectral region from 10 μm to 1 mm, initially developed for photochemical applications [29]. Unlike the electrical-discharge-pumped scheme, optically-pumped gas lasers greatly simplify the laser configuration and usually stand out in terms of high power conversion efficiency. Up to 28% conversion efficiency was reported in a continuous-wave (CW) NH_3 laser at 12.8 μm via a resonance-enhanced Raman scattering process pumped by CO_2 laser source [30]. Due to the nature of gaseous molecule absorption, the development of optically-pumped molecular gas lasers has been dependent on other gas lasers of rich emission spectral lines (commonly CO_2 lasers) as the pump source, which has limited the development of optically-pumped gas laser.

Today the rapid progress of solid-state lasers and fiber laser sources have provided various new coherent light sources of high performance combining wavelength tunability, narrow linewidth and high power, e.g., optical parametric oscillator/amplifiers, distributed Bragg reflector diode lasers, quantum cascade lasers and high-power fiber lasers. However, traditional gas lasers based on a simple capillary waveguide have not benefitted from these technologies that mainly cover the near-infrared wavelength region below 2 μm. This is because of the high loss of capillary waveguides used in optical-pumped gas lasers at those long wavelengths [31]. For example, in a capillary with a bore diameter of 100 μm the attenuation of fundamental mode is about 15 dB/m at a wavelength of 1 μm and 137 dB/m at 3 μm. Today we can address this problem with the emergence of anti-resonant HCFs. The emerging gas hollow core fiber lasers exhibit advantages of gas lasers in terms of the broad laser emission spectral range owing to a rich selection of gaseous gain media, and potential to achieve much higher-power emission. Optically-pumped HCF lasers can fill some spectral gaps where rare-earth-ion-doped fiber lasers fail to deliver [11], by using fiber laser pump sources.

C. Acetylene Fiber Laser for 3 μm Wavelengths

Acetylene was used as the gain medium in the first optically-pumped gas fiber laser in 2011 [32]. By using nanosecond pulses from an Optical Parametric Oscillator to pump at 1.52 μm wavelength, two mid-infrared emissions at 3.12 and 3.16 μm were observed in a 'Kagome' type of anti-resonant HCF filled with acetylene in a single-pass configuration [32]. Due to a high fiber loss (20 dB/m) at the laser wavelengths, the output power was low [32].

In 2013, by using an 11 m anti-resonant HCF with losses reduced to less than 0.2 dB/m at both pump and laser wavelengths, over 0.7 μJ pulsed laser emission around 3 μm was measured in a single-pass configuration with 30% power conversion efficiency pumped by a diode laser system at 1.53 μm [33]. Gas pressure was found to play a decisive role in the efficient laser

operation [33], [34], as in the earlier studies of traditional optically pumped gas lasers [29]. Recently, by pumping with a narrow-bandwidth OPA at 1.53 μm wavelength, 1.4 μJ pulse energy at 3 μm was obtained using a 10 m long acetylene-filled anti-resonant HCF in single-pass configuration [12]. A constant 20% slope efficiency was reported to be unaffected by the acetylene pressure [12] which may be a feature of lasing in the transient regime [13]. The M^2 of the output beam was measured as 1.2 [12].

The first cavity-based mid-infrared laser oscillation in acetylene-filled hollow fiber was realized in a ring cavity by a synchronous diode-pumping scheme [23]. 101 m of low-loss anti-resonant HCF was used as a feedback fiber with 25 dB/km fiber loss at 3 μm [23]. A maximum of over 4 mW average power was recorded at a repetition rate of 2.5 MHz [23]. In the same paper, the first CW lasing of acetylene molecules at 3 μm was also observed under CW diode laser pumping in the cavity configuration [23]. Later, we investigated acetylene gas lasing in the cavity and single-pass configurations under high-power pump well above lasing threshold [35], which demonstrated that the single-pass configure was preferred for high-power operation. Recently, we realized over 1 Watt mid-infrared laser output at 3 μm wavelengths under CW amplified diode laser system pumping [13]. Over 33% conversion efficiency was measured in a 15 m anti-resonant HCF in a single-pass configuration [13], relative to the absorbed pump power.

In this paper, we compare CW operation of optically-pumped acetylene HCF lasers in cavity and single-pass configurations based on both previously published data and our latest experimental results. By analyzing the power scaling and pump absorption of the laser, we demonstrate that the dynamics of the gain molecules constrains the laser performance under high-power CW pump. Both the need for low gas pressure and the reduced pump absorption of acetylene under high-power pumping necessitate use of long fiber lengths to maximize laser output power. Therefore, the low fiber attenuation is key to further increasing the CW output powers of optically-pumped acetylene HCF lasers.

II. ACETYLENE GAS AS GAIN MEDIUM

Acetylene gas has been widely used for wavelength calibration in the telecommunication band around at 1.53 μm because of the strong absorption lines at telecommunication wavelengths which arise due to the ro-vibrational transitions from the ground level to the $v_1 + v_3$ vibrational level [36]. Jones *et al.* reported that 3 μm photons could be emitted by the excited acetylene molecules transiting from the $v_1 + v_3$ vibrational state to the v_1 vibrational state [32]. Fig. 1 inset shows the energy diagram of acetylene energy levels for 3 μm emissions when pumped at the 1.5 μm absorption band. The P(9) absorption line from the v_0 ground vibrational state to the $v_1 + v_3$ vibrational state is ideal because of its high thermal population and large absorption cross-section. By pumping P(9), the $J = 8$ rotational state of $v_1 + v_3$ vibrational state is populated; and according to the selection rules, the excited molecules are allowed to transit to the $J = 7$ and $J = 9$ rotational states of v_1 vibrational state,
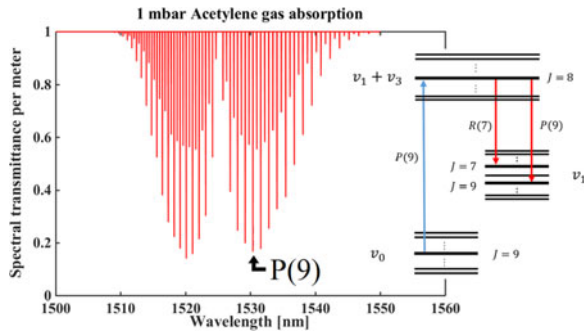
Fig. 1. Simulated absorption of acetylene gas in 1.5 μm spectral region at 20 °C using data from the HITRAN database [37]. For 1 mbar pressure, the linewidth is assumed decided by the Doppler broadening only. Inset: Energy diagram of acetylene energy levels for 3 μm emissions when pumped at P(9).
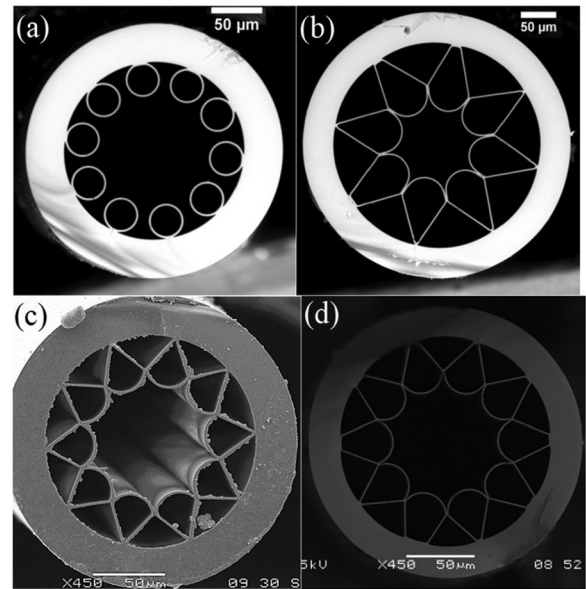

Fig. 2. Low-loss anti-resonant HCFs developed for acetylene HCF laser. (a) Anti-resonant HCF used as gain fiber filled with acetylene in the ring cavity [23]. (b) Anti-resonant HCF used as feedback fiber in the ring cavity [23]; 25 dB/km attenuation was measured at 3 μm. (c) Anti-resonant HCF used in the single-pass configuration [35]. (d) Anti-resonant HCF used in the single-pass configuration with the most balanced losses at pump and laser wavelengths [13]. The core sizes of (a)–(d) are approx. 109 μm, 88 μm, 72 μm and 72 μm respectively.

giving the R(7) and P(9) emissions respectively, which are at 3.12 and 3.16 μm. In this paper, all laser performance characterization and measurement were recorded by pumping at the P(9) wavelength (1530.385 nm).

It is noted that the transition from the v_1 vibrational state to the ground state is dipole forbidden [38], so that non-radiative relaxation plays an important role in CW lasing of acetylene molecules. A possible radiative route to depopulate the laser lower-level was indicated in [39] but no experimental observation was reported. Han *et al.* reported a removal rate of 12.3×10^{-10} cm^{3}s^{-1} that reflects the relaxation of population on $v_1 + v_3$ to neighboring states via vibrational and rotational energy transfer processes [40].

Doppler broadening dominates the linewidth of acetylene gas in anti-resonant HCF for 1 mbar pressure or less, where the mean-free-path of molecules is longer than the hollow core diameter at the room temperature [33]. As the pressure increases, the pressure broadening coefficient is about 9 MHz/mbar [36]. Fig. 1 shows the reconstructed acetylene absorption when the Doppler broadening dominates at 1 mbar pressure.

III. LOW-LOSS ANTI-RESONANT HCFs FOR OPTICAL PUMPED ACETYLENE LASING GENERATION

Since 2011 when the first low-loss silica-based anti-resonant hollow-core fiber was demonstrated at 3.5 μm wavelength and above [41], various types of anti-resonant HCFs have been proposed [19], [42], and tens of dB/km or even lower fiber attenuations of anti-resonant HCFs been reported for various spectral regions from UV [43] to mid-infrared wavelengths up to 4 μm [19].

Anti-resonant HCFs are leaky waveguides, and the total internal reflection model fails because of the reversal of refractive index contrast (low index air core and high index solid cladding). Leakage of light from the core is reduced by use of an anti-resonant reflection layer core wall, which is well explained by the ARROW model [44]. Such layer is regarded as a Fabry-Perot resonator at the glancing incidence. At the resonance wavelengths, light simply leaks out through the core wall into the surroundings, which defines the resonant loss region between low-loss transmission bands. Off resonance, the multiple-interference at the core wall reflects most of the light

back into the core and confines it to the fiber. On one hand, the anti-resonant cladding design can be used with large core sizes which reduces the fiber attenuation and dispersion and increases the optical damage threshold. On the other hand, the large-core design and curved core wall shape further reduce the core mode overlap with the fiber material (up to 10^{-4}) [20], [21] so that the fiber material loss and optical nonlinearity are reduced. Meanwhile, in contrast to photonic bandgap fibers, the simple fiber structure provides more flexibility in fiber design to fine tune for better optical properties, e.g., broadband single-mode performance [45] and low bend loss [46], *et al.* These merits make anti-resonant HCFs the most promising candidates for high-power/ultrafast laser delivery [47].

We have developed three types of anti-resonant HCFs for the optically-pumped acetylene fiber laser as shown in Fig. 2. Neighboring fiber transmission bands are used for pump and laser light transmission. Attenuation of the fiber shown in Fig. 2(b) is 25 dB/km at 3 μm [23], which is the lowest loss at this wavelength reported so far. However, due to the higher loss of this fiber (over 0.5 dB/m) at the 1.53 μm pump wavelength [23], the fiber in Fig. 2(b) was only implemented as the long length feedback fiber in a ring cavity configuration and is not ideal as a gain fiber. The 10-cell cladding design of anti-resonant HCF has exhibited the most balanced loss performance for simultaneous pump and laser light transmission. An early 10-cell cladding anti-resonant HCF (Fig. 2(c)) was reported to have 0.1 dB/m and 0.12 dB/m fiber attenuations at 1.53 μm and 3.1 μm respectively [35]. Later we reduced the fiber losses to 37 dB/km and 70 dB/km at pump and laser wavelengths [13],
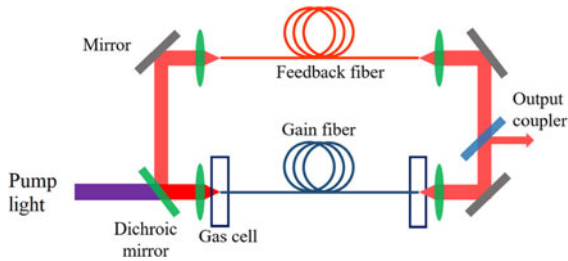
Fig. 3. A generic ring-cavity configuration of acetylene HCF laser.

which corresponds 42 m fiber length with less than 1.6 dB and 3 dB losses at pump and laser wavelengths respectively.

IV. RING-CAVITY CONFIGURATION

Acetylene HCF lasers have been extensively explored in the ns pulsed region since first proposed in 2010 [11], [32]–[34]. Due to the nature of low-pressure gas absorption, many efforts were devoted to the development of narrow-band pump sources with high power at 1.5 μm wavelength [12], [34]. One factor slowing the development of CW laser technology using more mature telecoms-based pump sources was a concern that the acetylene laser could self-terminate in CW operation because of a lack of rapid (radiative) relaxation routes to effectively depopulate the laser lower level. Another is the limitation of high-power fiber-based amplifiers for narrow-linewidth sources as a consequence of stimulated Brillouin scattering.

CW operation of acetylene HCF laser was first observed in a ring-cavity configuration, which was initially designed to achieve the laser oscillation in the pulsed region [23]. Fig. 3 shows a generic acetylene HCF laser based on a ring-cavity configuration adopted in [23], [35]. The introduction of feedback fiber was to reduce the laser threshold and establish the genuine laser oscillation [23]. In experiment, over 100 m low-loss anti-resonant HCF was used as the feedback fiber for a synchronously pumped scheme. As expected, the power conversion efficiency increased as the repetition rate of pump approached the characteristic frequency of the ring cavity. It was noted that the laser oscillation at 3 μm did not completely disappear at pump repetition rates away from the cavity frequency and harmonics, which implied a potential for CW operation. By using a shorter feedback fiber (3 m), the CW running state of acetylene anti-resonant HCF laser was first experimentally observed by CW diode laser pumping and the power conversion efficiency reached 6.7%, comparable with the maximum 8.8% in the pulsed region of cavity configuration [23].

Feedback in the ring-cavity configuration was found key to achieve laser generation near the threshold in both CW and pulsed regions [23]. However, well above the laser threshold, the introduction of feedback becomes a barrier impeding the extraction of full optical power [35]. At 0.6 mbar pressure, the power conversion efficiencies were 12.4% and 18.6% with and without feedback [35]. The ratio of slope efficiencies with and without feedback are nearly constant around 0.65, close to the 70% reflectivity of output coupler at 3.1 μm wavelengths [35]. It indicates that well above the laser threshold, the
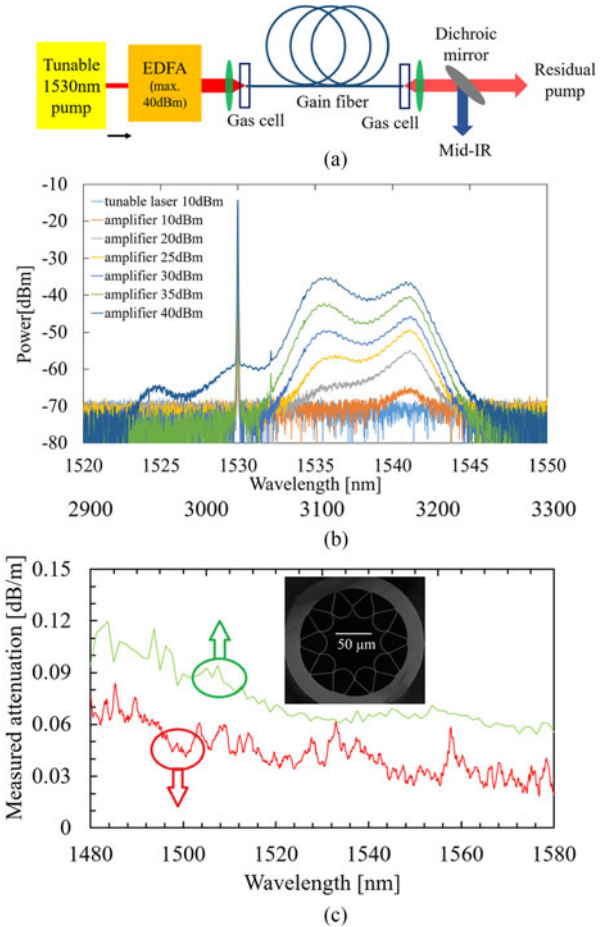

Fig. 4. (a) Schematic of single-pass configuration. (b) Measured spectra of EDFA output when the seed laser is tuned at P(9) wavelength. (c) Measured attenuation of anti-resonant HCF shown in Fig. 2(d) at both pumping and lasing wavelengths: 37 dB/km at 1.53 μm, 63 dB/km and 69 dB/km at 3.12 μm and 3.16 μm. Part of data in Fig. 4 are included [13].

ring-cavity configuration of acetylene HCF laser does not benefit laser output power but is simply an additional source of loss.

V. SINGLE-PASS CONFIGURATION

Fig. 4(a) presents a schematic of single-pass configuration of acetylene HCF laser. The pump source comprises a tunable DBR diode laser as seed (ID Photonics GMBH, CoBrite DX1, maximum power 40 mW, linewidth 100 kHz) and a customized high-power EDFA (Bktel Photonics, HPOA-S370ac). The measured spectra of EDFA output are shown in Fig. 5(b) when the seed laser is tuned to the P(9) line. The maximum output of the EDFA is 9.6 W (with a strong ASE background) of which about 4.9 W is measured to be absorbed by acetylene in a 31 m length of anti-resonant HCF at pressure of 0.6 mbar. Therefore roughly 50% of the EDFA output power can be regarded as the effective pump power for acetylene to absorb at the P(9) wavelength.

The anti-resonant HCFs in Fig. 2(c) and (d) were both used in the single-pass configuration [13], [35]. In this section, all presented measurements of acetylene HCF laser is based on use of the anti-resonant HCF shown in Fig. 2(d) which has the
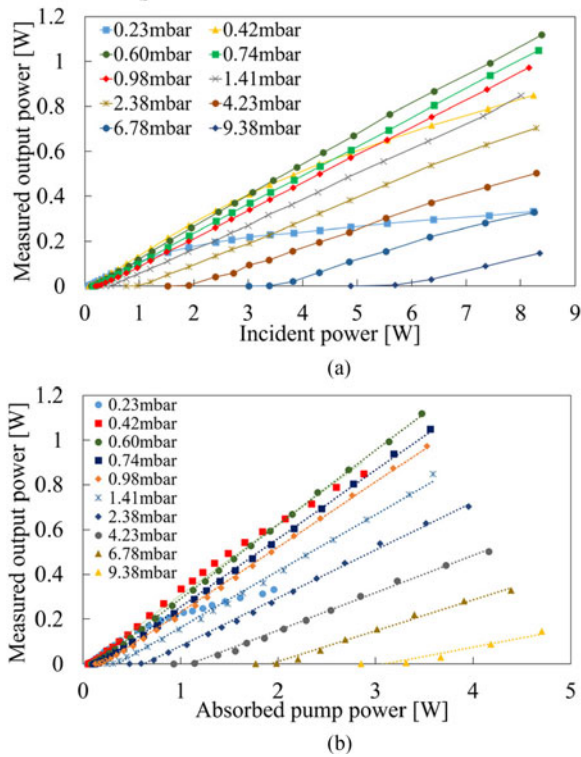
Fig. 5. For 15 m fiber length and different pressures, measured acetylene HCF laser output at 3 μm as a function of (a) total incident pump power (b) absorbed pump power at P(9) line. Part of data in Fig. 5 are included in [13].

Fig. 6. For 6 m, 15 m and 40 m fiber lengths, (a) measured maximum 3 μm laser output power for different gas pressures; (b) measured laser threshold (absorbed pump power) for different gas pressures. Part of data in Fig. 6 are included in [13].

lowest combined attenuations at pump and laser wavelengths (Fig. 5(c)) reported so far [12], [13], [32]–[35].

The coupling efficiency of pump light into the anti-resonant HCF is generally above 90% using a coated CaF$_2$ lens with 50 mm focus length. A dichroic mirror (94% transmission at 1.53 μm, 99% reflection at 3.16 μm) is used after the gain fiber output end to separate the residual pump light/ASE from the mid-IR output for measurement. A long-pass filter is used to further remove residual pump light before the 3 μm laser power is measured by the thermal detector (Ophir VEGA).

In fact, measurements of the pump transmission (tuned off P(9) line) combined with this measured attenuation value can only be explained by assuming 100% pump coupling efficiency, indicating that the actual attenuation might be somewhat lower than the value measured using a white light source.

A. Power-Scaling of Acetylene HCF Laser

Anti-resonant HCFs have been successfully demonstrated for high-power laser delivery [47], having higher damage threshold and reduced optical nonlinearity compared to conventional solid fibers. The improved power handling suggests that gas fiber lasers based on anti-resonant HCFs have the potential to deliver a higher power output than solid fiber lasers. In contrast to solid fiber lasers/amplifiers, the limit of gas HCF lasers in high-power laser generation is more likely determined by the power range of available pump sources of narrow linewidth rather than the constraints from HCFs as hosts of gain media. As a fiber gas laser, the density of gas as gain for lasing could be flexibly and
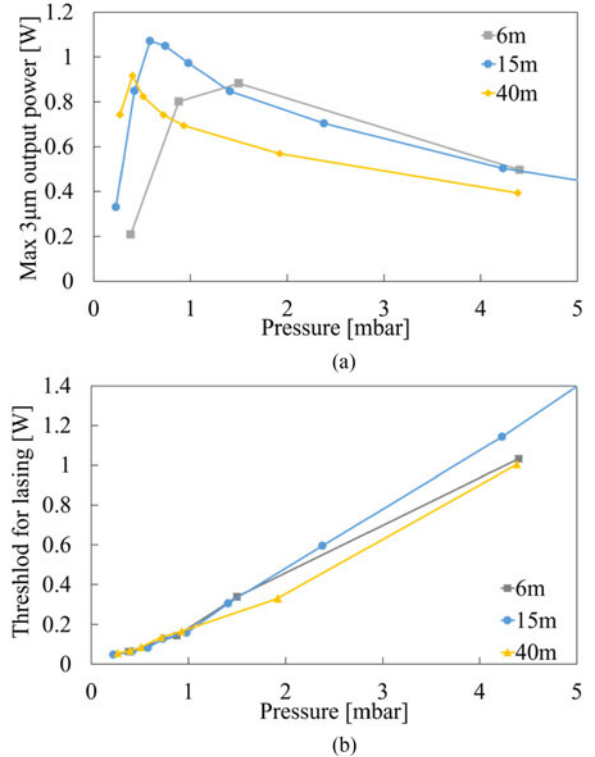
conveniently adjusted in a broad range along the fiber length. This merit provides a new freedom in optimization of fiber laser performance for high-power laser generation, which is difficult to achieve in its counter-parts of rare-earth-ions doped solid fiber lasers.

Fig. 5 show the power scaling of acetylene HCF laser for 15 m fiber length at different pressure against (a) the total incident pump power including effect pump and ASE from EDFA and (b) the absorbed pump power at P(9) line. The maximum output power at 3 μm was measured as 1.12 W with the maximum power conversion efficiency of 33.2% at 0.6 mbar relative to the absorbed pump. At lower pressures of 0.23 mbar and 0.42 mbar, gain saturation was observed; whereas at pressures higher than 0.6 mbar, the laser output decreased with pressure.

The dependences of power conversion efficiencies on acetylene gas pressure for different fiber lengths were found of similar trend. Fig. 6 summarizes (a) measured 3 μm laser output power under full-power incident pump and (b) measured laser threshold as functions of acetylene gas pressure, for three fiber lengths. For 6 m and 40 m, the maximum laser outputs were recorded as 0.8 W and 0.92 W at 0.88 mbar and 0.42 mbar, with the slope efficiency of 28% and 31.2% respectively.

This similar dependences of power scaling for different fiber lengths on gas pressure imply the pressure-induced dynamics of acetylene molecules inside HCF underlies the gain performance of laser. The acetylene pressure is a macroscopic measure of molecular collisions inside the fiber including inelastic

collisions with the core wall to dissipate the pump energy into environment and inter-molecular collisions to realize vibrational/rotational energy transfer. As discussed in Section II, the pressure-induced dynamics of acetylene molecules is key to maintain the efficient CW operation of acetylene given lack of radiative relaxation routes for laser lower level.

The $J = 8$ rotational state of $v_1 + v_3$ vibrational state has been reported to be depopulated at a total removal rate of $12.3 \times 10^{10}\,\mathrm{cm^3 s^{-1}}$ (measured when pressure lower than 0.4 mbar) in [40], by the vibrational and rotational energy transfer processes via intermolecular collisions. Unlike in free space, the inelastic collisions with the core wall of acetylene molecules confined in HCF also make a significant contribution to, or even dominate, the relaxation processes, which equally depopulate the laser upper and lower levels, in the extremely low pressure region less than 2.1 mbar where the mean free path of molecules is smaller than the fiber core radius (36 μm). The reduced gain at higher pressure is clearly shown in Fig. 6(b) near the laser threshold: for a fixed fiber length, the laser threshold increases almost linearly with the pressure. However, under pump powers sufficiently above the threshold, the reduced lifetime of excited acetylene molecules can be compensated by the higher molecule density in a certain range of pressure and the net gain can be possibly maintained or even increased. It is noted that, when the depopulation rate overwhelms the advantage of high molecular density, the net gain of acetylene gas ultimately decreases as shown in Fig. 6(a). The maximum output power is obtained when the pressure is such as to absorb the maximum pump power without leading to a significant decrease in gain as a consequence of collisional de-excitation.

In the experiments, for 6 m fiber length, gain saturation was observed under full incident pump power for all acetylene pressures less than 0.88 mbar with the effective pump power being partially absorbed. For 40 m fiber length, no saturation could be observed at pressure less than 0.4 mbar at any pump power.

In the quasi-CW region, a similar dependence of laser power-scaling performance on acetylene pressure has been also confirmed for pulsed pump of tens of ns pulse durations [23], [33], [34]. When the pulse width is shortened to approximately 1 ns, a constant 20% slope efficiency was observed instead for a pressures range from 1.6 mbar to 18.7 mbar [12]. As the pump pulse length becomes shorter entering the transient region, when the pump duration becomes shorter than the collisional kinetic process, it is reasonable to assume that collision-induced changes barely take place (over a certain pressure range) in the short pulse duration of pumping. In that case, the limited fraction of acetylene molecules which can participate in the lasing process is mainly decided by the thermal equilibrium distribution. As a result, a higher pressure may be preferable for more effective utilization of pump power for extremely short durations.

B. Output Spectra of Acetylene HCF Laser

As shown in the transition diagram (Fig. 1 inset), R(7) and P(9) transitions from the $v_1 + v_3$ vibrational state to the v_1 vibrational state can emit at 3.12 μm and 3.16 μm wavelengths when pumping at P(9) line from the ground level and the $v_1 + v_3$
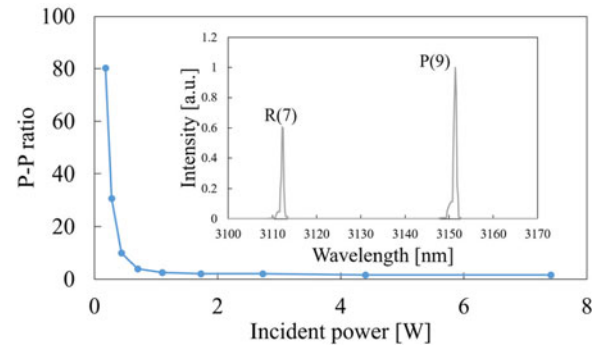

Fig. 7. The ratio of laser peak intensity via P(9) transition over the one via R(7) transition as a function of the incident power. Inset: measured typical laser output optical spectrum (not resolved). About 10 nm spectral offset is found in measurements of laser lines which we attribute to the calibration error of our monochromator at 3 μm wavelengths. All spectral data was recorded at 0.6 mbar pressure for the 15 m fiber length. The laser spectra in the cavity configuration were found to be similar to that shown inset.

vibrational state. All the measured mid-infrared laser output powers at 3 μm in Figs. 6 and 7 do not distinguish between these two laser wavelengths. To characterize the output spectra, a short piece ($\sim$1 m) of low-loss anti-resonant HCF with low attenuations from 3 μm to 4 μm was used to sample laser output to be measured by a monochromator (Bentham TMc300).

Fig. 7 plots the ratios of measured peak intensities at two laser wavelengths for different incident pump powers, at the optimized acetylene pressure of 0.6 mbar for 15 m fiber length. Just above the laser threshold, P(9) emission dominates the output. At higher pump powers both lines are observed and their ratio quickly reaches a steady state.

It is noted that no other emission lines of acetylene HCF laser have been reported when pumping at one single ro-vibrational transition line around 1.5 μm wavelengths, in the pulsed or CW region [12], [32]–[34]. It implies that neither the rotational nor vibrational energy transfer via inter-molecular collisions should be efficient enough to depopulate the excited ro-vibrational state of laser upper level to its neighbor states to achieve significant population inversion for stimulated emissions at any new wavelengths.

C. Characterization of Pump Absorption

To characterize the pump absorption we adopted the side-scattering measurement to investigate the transmitted pump light along the fiber length. The pump light lost from the fiber core will leave the fiber through the side walls. By collecting some of light locally using a standard multimode fiber, we can analyze it with an optical spectrum analyzer (YOKOGAWA AQ6370). Fig. 8(a) shows typical spectra measured from the fiber side, when the seed laser is tuned at and off P(9) lines (on/off absorption resonance) of acetylene. The ratio of peak intensities on and off resonance is used to quantify the pump absorption for the measured position along the fiber.

Fig. 8(b) shows the pump absorption along 15 m fiber length at 0.6 mbar pressure under different incident pump powers. The slope of longitudinal absorption is found reduced as the incident power increases. In the steady state, for a constant gas density,
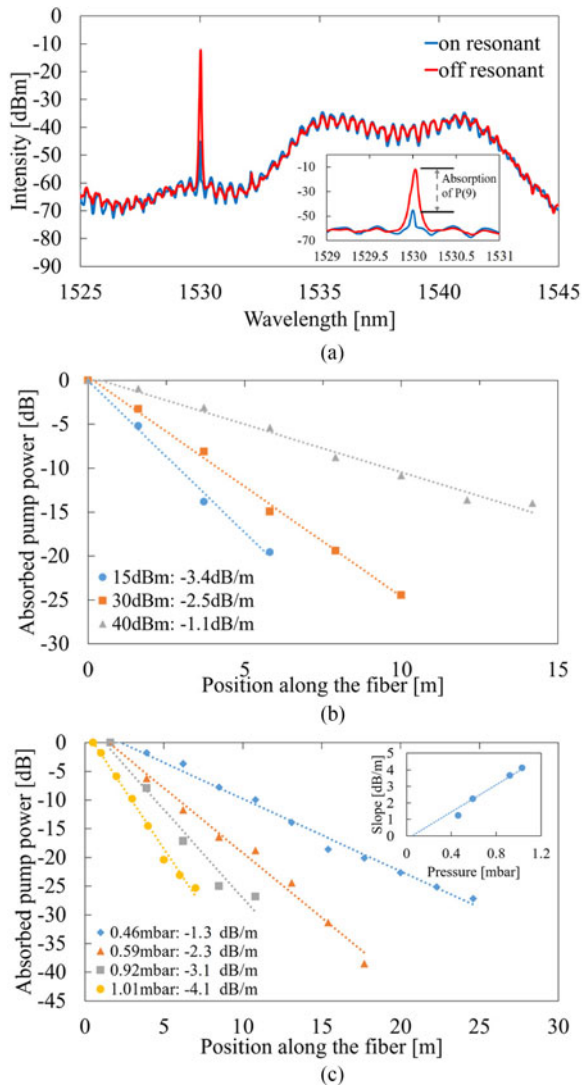
Fig. 8. (a) Typical measured spectra of the pump light at P(9) on/off resonant wavelength. The ratio of the peak intensities represents the relative absorbed pump power through the measured fiber length. (b) Pump absorption as a function of the longitudinal position along the 15 m fiber at 0.6 mbar pressure for different incident powers (15 dBm, 30 dBm and 40 dBm). (c) Pump absorption as a function of the longitudinal position along the 31 m fiber with the full incident pump power for different gas pressures. Part of data in Fig. 8 are included in [13].

the pump absorption is dependent on the population distributions of ground level and laser upper level. As the power pump is increased, more molecules participate in the stimulated emission processes while the ground level will be quickly depopulated, reducing the pump absorption due to shelving in intermediate states. As the pump further increases, the gain saturation can be expected. Therefore, a longer fiber length is required for higher-power generation under sufficient pump power.

For a fixed fiber length, higher acetylene pressure increases the absorption as shown in Fig. 8(c). The inset shows the longitudinal pump absorption as a function of the pressure, with 4.12 dB/m/mbar slope fitting. The increase of pump absorption with pressure is attributed to both higher molecule density and faster depopulation of laser upper/lower levels because of collisions.

However, as demonstrated in Figs. 5 and 6, the increased pump absorption at high pressure does not naturally come with higher gain or power conversion. For a fixed length, the low pressure condition provides the highest power conversion efficiency.

The reduced pump absorption under high-power pump and the reduced laser output generation under higher pressure both suggest a long fiber length filled with low-pressure acetylene is key to efficient CW laser operation and high-power laser generation, necessitating the further development of anti-resonant HCFs and novel HCFs with improved loss performance.

VI. CONCLUSION

In summary, we review the studies of CW acetylene HCF laser for 3 μm wavelength in both ring-cavity and single-pass configurations. We systematically characterize acetylene HCF laser in aspects of power-scaling, laser output spectra and pump absorption. We find that a ring cavity can offer the lowest laser threshold but that high efficiency at high pump powers is best achieved using a single-pass configuration. Over 1 Watt output power at 3 μm is reported as the maximum power with a slope efficiency of over 33% at 0.6 mbar in 15 m anti-resonant HCF. We discover that the molecular dynamics inside the gain fiber determines the laser performance and that further improvement in the loss performance of HCF would be required to achieve higher-power laser generation at 3 μm wavelengths. The potential for higher power laser generation in acetylene gas fiber lasers can be realized by using a higher pump power and longer length of anti-resonant HCF with lower loss. To achieve this lower loss a larger core diameter and novel fiber design may be needed.

All data underlying the results presented in this letter can be found at [48].

REFERENCES

[1] X. Zhu and N. Peyghambarian, "High-power ZBLAN glass fiber lasers: Review and prospect," *Adv. Optoelectron.*, vol. 2010, 2010, Art. no. 501956.

[2] S. D. Jackson, "Towards high-power mid-infrared emission from a fibre laser," *Nature Photon.*, vol. 6, no. 7, pp. 423–431, Jun. 2012.

[3] M. C. Falconi, D. Laneve, and F. Prudenzano, "Advances in Mid-IR Fiber lasers: Tellurite, fluoride, and chalcogenide," *Fibers*, vol. 5, no. 2, 2017, Art. no. 23.

[4] R. Kitamura, L. Pilon, and M. Jonasz, "Optical constants of silica glass from extreme ultraviolet to far infrared at near room temperature," *Appl. Opt.*, vol. 46, no. 33, Nov. 2007, Art. no. 8118.

[5] G. Tao *et al.*, "Infrared fibers," *Adv. Opt. Photon.*, vol. 7, no. 2, Jun. 2015, Art. no. 379.

[6] V. Fortin *et al.*, "Watt-level erbium-doped all-fiber laser at 3.44 μm," *Opt. Lett.*, vol. 41, no. 3, 2016, Art. no. 559.

[7] O. H. Sapir, S. D. Jackson, and D. Ottaway, "Versatile and widely tunable mid-infrared erbium doped ZBLAN fiber laser," *Opt. Lett.*, vol. 41, no. 7, pp. 1676–1679, 2016.

[8] O. Henderson-Sapir *et al.*, "Recent advances in 3.5 μm Erbium-Doped Mid-Infrared fiber lasers," *IEEE J. Sel. Topics Quantum Electron.*, vol. 23, no. 3, pp. 6–14, May 2017.

[9] Y. O. Aydın *et al.*, "Diode-pumped mid-infrared fiber laser with 50% slope efficiency," *Optica*, vol. 4, no. 2, 2017, Art. no. 235.

[10] F. Maes, V. Fortin, M. Bernier, and R. Vallée, "5.6 W monolithic fiber laser at 3.55 μm," *Opt. Lett.*, vol. 42, no. 11, pp. 2054–2057, 2017.

[11] A. V. V. Nampoothiri *et al.*, "Hollow-core Optical Fiber Gas Lasers (HOF-GLAS): A review [Invited]," *Opt. Mater. Express*, vol. 2, no. 7, pp. 948–961, Jun. 2012.

[12] N. Dadashzadeh *et al.*, "Near diffraction-limited performance of an OPA pumped acetylene-filled hollow-core fiber laser in the mid-IR," *Opt. Express*, vol. 25, no. 12, Jun. 2017, Art. no. 13351.

[13] M. Xu, F. Yu, and J. C. Knight, "Mid-infrared 1 Watt hollow-core fiber gas laser source," *Opt. Lett.*, vol. 42, no. 20, pp. 4055–4058, 2017.

[14] R. F. Cregan, "Single-Mode photonic band gap guidance of light in air," *Science*, vol. 285, no. 5433, pp. 1537–1539, 1999.

[15] P. S. J. Russell, "Photonic-crystal fibers," *J. Lightw. Technol.*, vol. 24, no. 12, pp. 4729–4749, Dec. 2006.

[16] P. J. Roberts *et al.*, "Ultimate low loss of hollow-core photonic crystal fibres," *Opt. Express*, vol. 13, no. 1, Jan. 2005, Art. no. 236.

[17] P. J. Mosley *et al.*, "Ultrashort pulse compression and delivery in a hollow-core photonic crystal fiber at 540 nm wavelength," *Opt. Lett.*, vol. 35, no. 21, pp. 3589–3591, 2010.

[18] Y. Kawaguchi, Y. Tamura, T. Haruna, Y. Yamamoto, and M. Hirano, "Ultra low-loss pure silica core fiber," *SEI Tech. Rev.*, no. 80, pp. 50–55, 2015.

[19] F. Yu and J. Knight, "Negative curvature hollow-core optical fiber," *IEEE J. Sel. Topics Quantum Electron.*, vol. 22, no. 2, Mar./Apr. 2015, Art. no. 4400610.

[20] F. Yu and J. C. Knight, "Spectral attenuation limits of silica hollow core negative curvature fiber," *Opt. Express*, vol. 21, no. 18, pp. 21466–21471, Sep. 2013.

[21] W. Belardi and J. C. Knight, "Effect of core boundary curvature on the confinement losses of hollow antiresonant fibers," *Opt. Express*, vol. 21, no. 19, pp. 21912–21917, Sep. 2013.

[22] F. Yu, W. J. Wadsworth, and J. C. Knight, "Low loss silica hollow core fibers for 3-4 μm spectral region," *Opt. Express*, vol. 20, no. 10, pp. 11153–11158, May 2012.

[23] M. R. A. Hassan, F. Yu, W. J. Wadsworth, and J. C. Knight, "Cavity-based mid-IR fiber gas laser pumped by a diode laser," *Optica*, vol. 3, no. 3, Mar. 2016, Art. no. 218.

[24] M. F. Churbanov, G. E. Snopatin, V. S. Shiryaev, V. G. Plotnichenko, and E. M. Dianov, "Recent advances in preparation of high-purity glasses based on arsenic chalcogenides for fiber optics," *J. Non-Cryst. Solids*, vol. 357, no. 11–13, pp. 2352–2357, 2011.

[25] [Online]. Available: https://www.fiberlabs-inc.com/fiberindex/fiber-stock/

[26] A. Urich *et al.*, "Flexible delivery of Er:YAG radiation at 2.94 μm with negative curvature silica glass fibers: a new solution for minimally invasive surgical procedures," *Biomed. Opt. Express*, vol. 4, no. 2, pp. 193–205, Feb. 2013.

[27] A. Urich *et al.*, "Delivery of high energy Er: YAG pulsed laser light at 2.94 μm through a silica hollow core photonic crystal fibre," *Opt. Express*, vol. 20, no. 6, pp. 6677–84, 2012.

[28] F. Yu, M. Xu, and J. C. Knight, "Experimental study of low-loss single-mode performance in anti-resonant hollow-core fibers," *Opt. Express*, vol. 24, no. 12, Jun. 2016, Art. no. 12969.

[29] P. K. Gupta and S. C. Mehendale, "Mid-infrared optically pumped molecular lasers," *Hyperfine Interact.*, vol. 37, pp. 243–274, 1987.

[30] C. Rolland, J. Reid, and B. K. Garside, "10-W cw optically pumped 12 μm NH_3 laser," *Appl. Phys. Lett.*, vol. 44, no. 8, pp. 725–727, Apr. 1984.

[31] J. J. Degnan, "The waveguide laser: A review," *Appl. Phys.*, vol. 11, no. 1, pp. 1–33, 1976.

[32] A. M. Jones *et al.*, "Mid-infrared gas filled photonic crystal fiber laser based on population inversion," *Opt. Express*, vol. 19, no. 3, pp. 2309–2316, Jan. 2011.

[33] Z. Wang, W. Belardi, F. Yu, W. J. Wadsworth, and J. C. Knight, "Efficient diode-pumped mid-infrared emission from acetylene-filled hollow-core fiber," *Opt. Express*, vol. 22, no. 18, pp. 21872–21878, Sep. 2014.

[34] Z. Wang, Z. Zhou, Z. Li, N. Zhang, and Y. Chen, "Tunable mid-infrared emission from acetylene-filled hollow-core fiber," *Proc. SPIE*, vol. 10030, 2016, Art. no. 1003013.

[35] M. Xu, F. Yu, M. R. Hassan, and J. Knight, "Continuous-Wave 3.1 μm Gas fiber laser with 0.47 W output power," in *Proc. Conf. Lasers Electro-Opt.*, 2017, Paper SF2K.4.

[36] W. C. Swann and S. L. Gilbert, "Pressure-induced shift and broadening of 1510 nm–1540 nm acetylene wavelength calibration lines," *J. Opt. Soc. Amer. B*, vol. 17, no. 7, pp. 1263–1270, 2000.

[37] L. S. Rothman *et al.*, "The HITRAN2012 molecular spectroscopic database," *J. Quant. Spectrosc. Radiat. Transf.*, vol. 130, pp. 4–50, Nov. 2013.

[38] G. Herzberg, *Molecular Spectra and Molecular Structure. Volume II: Infrared and Raman Spectra of Polyatomic Molecules*. New York, NY, USA: Van Nostrand, 1945.

[39] A. M. Jones *et al.*, "C_2H_2 gas laser inside hollow-core photonic crystal fiber based on population inversion," in *Proc. Conf. Lasers Electro-Opt. 2010*, 2010, Paper CTuU1.

[40] J. Han, K. Freel, and M. C. Heaven, "Rotational and vibrational energy transfer in vibrationally excited acetylene at energies near 6560 cm(-1)," *J. Chem. Phys.*, vol. 135, no. 24, Dec. 2011, Art. no. 244304.

[41] A. D. Pryamikov *et al.*, "Demonstration of a waveguide regime for a silica hollow–core microstructured optical fiber with a negative curvature of the core boundary in the spectral region >3.5 μm," *Opt. Express*, vol. 19, no. 2, pp. 1441–8, Jan. 2011.

[42] F. Poletti, "Nested antiresonant nodeless hollow core fiber," *Opt. Express*, vol. 22, no. 20, 2014, Art. no. 23807.

[43] F. Yu, W. Wadsworth, and J. Knight, "Low-loss antiresonant hollow-core fiber for UV," in *Proc. Laser Congr. 2017*, 2017, Paper ATu5A.4.

[44] N. M. Litchinitser, A. K. Abeeluck, C. Headley, and B. J. Eggleton, "Antiresonant reflecting photonic crystal optical waveguides," *Opt. Lett.*, vol. 27, no. 18, Sep. 2002, Art. no. 1592.

[45] F. Yu, M. Xu, and J. C. Knight, "Experimental study of low-loss single-mode performance in anti-resonant hollow-core fibers," *Opt. Express*, vol. 24, no. 12, Jun. 2016, Art. no. 12969.

[46] Richard M. Carter *et al.*, "Measurement of resonant bend loss in anti-resonant hollow core optical fiber," *Opt. Express*, vol. 25, no. 17, pp. 20612–20621, 2017.

[47] J. D. Shephard *et al.*, "Silica hollow core microstructured fibers for beam delivery in industrial and medical applications," *Frontiers Phys.*, vol. 3, Apr. 2015, Art. no. 24.

[48] [Online]. Available: https://doi.org/10.15125/BATH-00406

Mengrong Xu was born in China, in 1991. She received the B.S. degree in measurement control technology and instruments from Shanghai Jiao Tong University, Shanghai, China, in 2012. She is currently working toward the Ph.D. degree in optics at the University of Bath, Bath, U.K. Her research interests include hollow core fiber optics and gas fiber lasers.

Fei Yu received the B.S. and M.S. degrees in physics electronics from the Beijing Institute of Technology, Beijing, China, in 2008 and 2010, respectively. He received the Ph.D. degree in optics from the University of Bath, Bath, U.K., in 2014. He is currently a Research Officer with the University of Bath. His research interests include optical fiber design and applications.

Muhammad Rosdi Abu Hassan received the B.Eng. and M.Sc. degrees from the University of Malaya, Kuala Lumpur, Malaysia, in 2009 and 2011, respectively, in the field telecommunication engineering and optical fiber-based sensors. He received the Ph.D. degree from the University of Bath, Bath, U.K., in 2017. He is currently a Postdoctoral Fellow with the Faculty of Engineering, Multimedia University, Cyberjaya, Malaysia. His current research interests include fiber gas laser, fiber fabrication, and fiber based sensors.

Jonathan C. Knight received the Ph.D. degree from Cape Town, and did the Postdoctoral Research with the Ecole Normale Superieure, Paris, France, and the University of Southampton, Southampton, U.K. He is currently a Professor with the Department of Physics, University of Bath, Bath, U.K., where he works on new forms of optical fibers and their applications.